Research Article

Roberto Benocci*, H. Eduardo Roman, Chiara Confalonieri, and Giovanni Zambon

Investigation on clusters stability in DYNAMAP's monitoring network during Covid-19 outbreak

https://doi.org/10.1515/noise-2020-0023
Received Oct 02, 2020; accepted Nov 04, 2020

Abstract: From March 23rd to May 3rd 2020, Italy underwent a complete lockdown in the attempt to contain the spread of the pandemic due to Covid-19 outbreak. During this period, a new kind of environment has been experienced in all cities, resulting in an abatement of traffic noise levels. Consequently, due to the prohibition of all non-essential activities, traffic noise dynamics changed as well. In this paper, we analyse the data recorded from the permanent noise monitoring network installed in the pilot area of the city of Milan, Italy. The results show how, besides a dramatic reduction of the noise levels (about 6 dB on average), also the noise pattern was profoundly changed. This is particularly important in the framework of DYNAMAP, a statistically based European project able to predict traffic noise over an extended area based on the noise recorded by limited number of monitoring stations. The change of the traffic dynamics, resulting in different noise patterns of the normalized hourly median profiles for each sensor, pose some limitations about the use of such predicting tool during extraordinary situations such as that experienced during a lockdown.

Keywords: noise mapping; cluster analysis; DYNAMAP; Covid-19; traffic noise pattern

***Corresponding Author: Roberto Benocci:** Dipartimento di Scienze dell'Ambiente e del Territorio e di Scienze della Terra (DISAT), Università di Milano-Bicocca, Piazza della Scienza 1, 20126 Milano, Italy; Email: roberto.benocci@unimib.it
H. Eduardo Roman: Dipartimento di Fisica, "G. Occhialini" Università di Milano-Bicocca, Piazza della Scienza 3, 20126 Milano, Italy
Chiara Confalonieri, Giovanni Zambon: Dipartimento di Scienze dell'Ambiente e del Territorio e di Scienze della Terra (DISAT), Università di Milano-Bicocca, Piazza della Scienza 1, 20126 Milano, Italy

1 Introduction

Noise maps are gaining increasing importance as means for evaluating the noise exposure of the population, especially after the publication of the Directive 2002/49/EC [1] and the 2018 WHO Environmental noise guidelines [2] reporting dose harmful effects of noise on health. Indeed, strategic maps and Action Plans represent a vigorous boost for noise prevention and control [3, 4] and have become a common tool for local intervention measures and policy-making [5, 6]. Noise mapping are rapidly progressing towards the description of more realistic scenarios through the implementation of techniques of sound source recognition, predictive models and vehicles speed assessment [7–14].

On this topic, long-term investigations in Europe have been undertaken by permanent monitoring across cities such as Madrid, Rome, Paris, Milan and Rotterdam [15–19].

In particular, the European project DYNAMAP [20], has been developed to capture the time variation of noise, thus accounting for a more realistic impact of noise exposure in large urban [18] and suburban areas [16]. DYNAMAP has a strong statistical structure that is displayed by the similar dynamic behaviour of roads making up the urban network. The idea that noise emission from a street generally depends on its activity, its use in the urban context rather than strictly from its geometric characteristics, suggested an approach based on a categorization method for the analysis of urban noise. It lies on the generally accepted assumption that road traffic is the most important source of noise in towns, and can therefore be considered the main cause of its spatial and temporal variability [21–23].

This concept arose by analysing the traffic noise recorded from 93 sites distributed all over the city of Milan [24]. The analysis showed that roads tend to agglomerate around two distinct temporal dynamics,

Group (a): Roads presenting a strong variation between day and night noise levels.
Group (b): Roads presenting less variation between day and night noise levels (similar noise levels during the whole day).

This behaviour is strictly correlated with a non-acoustic parameter, x, known for each road and associated to the logarithm of the total traffic flow (*i.e.* $x = \log T_t$). The latter is related to a model calculation of the traffic flow on that road stretch. Here, we have used the traffic model developed by the Municipal Agency for Mobility, Environment and Territory (Agenzia Mobilità Ambiente e Territorio, AMAT), in charge of the transportation policy in the city of Milan.

In this way, roads belonging to Group (a) have been found to be associated with a low value of x. Indeed, a low total traffic flow is generally found in roads presenting high traffic flow variability between day and night (local and secondary roads). Group (b) is mainly composed of roads with high x values. Roads with high capacity traffic flows belong to this group. Just as a reference value, a previous work showed that the "hard" threshold, x_h, between the two groups is $x_h = 4.45$ [25].

Therefore, each non-monitored road in principle can be associated with one of these two noise behaviours. DYNAMAP has been implemented in a pilot area consisting of about 2000 road segments, which can be attributed to one of the two clusters according to their known non-acoustic parameter.

The statistical character of DYNAMAP allows the use of a limited number of noise monitoring sensors (24 in this particular case) to capture the traffic dynamics variability within the pilot area. For convenience, the entire range of variability of the non-acoustic parameter has been divided into six groups (in principle, they are two), and each group of roads is represented by the same noise map. The latter is the result of two contributions:

(1) A reference static contribution obtained from the CadnaA software.
(2) A dynamic contribution retrieved from the 24 field monitoring stations [26].

The dynamic map of the whole pilot area is then obtained by energetically summing the static contribution of each map (1) and its dynamical variation (2).

As mentioned above, DYNAMAP is a dynamic noise mapping tool based on statistics able to generate a noise map on an extended area assuming that the mean noise trend profiles of each road in the mapped area remain stable. This paper is devoted to the analysis of the changes in the dynamic characteristics of the monitoring network of DYNAMAP in order to establish the validity of its prediction capability.

2 Materials and methods

The entire DYNAMAP network, built on 24 class 1 monitoring stations, has been used to investigate the noise level changes generated by the different sound sources over the studied period. In addition to this, we can count on a database of acoustic measurements recorded from August 2017 (DYNAMAP's kick-off). This is particularly important considering the aim of this research to compare the noise levels recorded during the lockdown and the same period in 2019. In the following, we present the analysis of the data recorded from all the monitoring stations. The recorded noise data refer to the periods corresponding to the Italian Government measures in reply to Covid-19 pandemic, and data treatment is specified according to our standards:

- Time interval
  Analysed period: weekdays from 23rd March to 3rd May 2020
  Reference period: weekdays from 23rd March to 3rd May 2019
- Data treatment
  Identification of missing data due to sensor offline or temporarily out of use.
  Removal of noise data for the hours of the day with unfavourable weather conditions (rain rate > 2 mm/h and wind speed > 5 m/sec) obtained by cross-checking ARPA Lombardia weather stations (see Table 2).
  Removal of non-traffic events (*e.g.* sirens, horns, airplane flyovers, noisy human activities, technical facilities, etc.) by means of a built-in Anomalous Noise Events Detector (ANED) algorithm [27, 28].

The dataset considered consists of recordings of 21 monitoring stations during (23rd March – 3rd May) 2019, and 22 monitoring stations during (23rd March – 3rd May) 2020. For this analysis, just the weekdays have been considered. We could not use all the (24) installed sensors since a few were offline. All the information regarding the employed monitoring stations are listed in Table 1. Since most of the monitoring sensors are mounted in proximity or at the façade, the ISO 1996-2 standard [29] proposes a series of conditions for the location of the microphone (annex B) and mentions an associated uncertainty for correction of noise levels due to the reflections if these requirements are not met [30]. Since the morphology of the façades in reality is very complex, it is difficult to fulfil all the requirements for in situ measurements. Therefore, to have a univocal and precautionary data on all the sites, it

Table 1: Information regarding the employed monitoring stations: Site address, sensor code, position, distance from center of track, obstacles and track width. All sensors are positioned at a 4 m height and they overlook traditional asphalt pavement

Site address	Sensor code	Sensor position	Distance between sensor and centre of the track [m]	Obstacles	Track width [m]	N° of total lanes
Via Litta Modignani	hb106	Building façade	16	No	13.5	2
Via Piero e Alberto Pirelli (U4)	hb108	Building façade	21	No	17	2
Viale Stelvio	hb109	Building façade	15	Trees	22.3	4
Via Melchiorre Gioia	hb114	Railing	18	No	30	4
Via Fara	hb115	Building façade	11	No	8	1
Via Moncalieri	hb116	Building façade	15	No	11	2
Viale Fermi	hb117	Building façade	35	Trees	30	6
Via Baldinucci	hb120	Building façade	10	Hedge	7	2
Via Piero e Alberto Pirelli (U6)	hb121	Building façade	9	No	17	2
Via Abba	hb125	Building façade	12	No	10	1
Via Quadrio	hb127	Building façade	8	No	6.5	1
Via Crespi	hb129	Building façade	12	No	13	2
Via Maffucci	hb133	Building façade	20	Trees	7	1
Via Lambruschini	hb135	Building façade	4	No	6.5	1
Via Comasina	hb136	Building façade	19	No	8	2
Via Maestri del lavoro	hb137	Building façade	6	No	8	1
Via Novaro	hb138	Railing	8	Trees	7.5	1
Via Bruni	hb139	Building façade	5	No	5	1
Viale Jenner	hb140	Building façade	15	No	32	4
Via D'Intignano	hb144	Railing	6	No	7	1
Via Fratelli Grimm	hb145	Building façade	14	No	7.5	1
Via Veglia	hb151	Building façade	9	No	10	2

Table 2: Average weather condition in the two analysed periods

	23rd March to 3rd May 2019	23rd March to 3rd May 2020
Number of analyzed weekdays	27	28
Number of rainy days (>2mm per day)	6	6
Average temperature [°C]	13.6 ± 2.1	13.2 ± 4.4

is possible to consider a correction of −6 dB, as indicated in ISO 1996-2 standard, for microphones installed flush with the wall.

The monitoring stations are periodically calibrated (once a year). The calibrator used is a class 1 model 4231 from Brüel & Kjær. The average weather conditions were approximately equivalent in both periods as reported in Table 2.

In order to get "robust" noise profiles, we calculated, for each sensor, its median value over the period of investigation. The median was chosen because it is less influenced by the presence of outliers. Due to the non-homogeneity of levels dataset, in particular as a result of varying monitoring conditions such as different distances from the road, and also to the characteristics of the street itself (its geometry, the presence of reflecting surfaces and obstacles in sound propagation and types of paving), each value of the temporal series was referred to the corresponding daytime level (Leq_{06-22}), taken as the reference value (normalization).

In this way, we analyse the noise profile of a specific sensor by focusing on its dynamic behaviour. In order to

reveal their different behaviours in the dataset, an unsupervised clustering algorithm has been applied to group together the hourly median level profiles. The following algorithms have been applied: Hierarchical agglomeration using Ward algorithm [31]; K-means algorithm [32]; Partitioning Around Medoids (PAM) [33]; DIvisive ANAlysis Clustering (DIANA) [33]; Self-organizing Tree Algorithm (SOTA) [34]; Clustering Large Applications (CLARA) [33]; AGglomerative NESting (Hierarchical Clustering) AGNES [33] and the corresponding results were compared. The range of solutions for clustering has been set from six groups to two, the latter corresponding to the minimal discrimination between the data. Euclidean distance has been chosen as the metric of the distance among observations. The open source software "R", version 1.2.5033 [35], has been applied for clustering and the package "clValid" [36, 37] has been used for validating the results of the different cluster algorithms. All the clustering algorithms have been ranked based on their performance as determined simultaneously by all the validation measures: internal and stability [38–43].

3 Results and discussion

In order to highlight the effects of the entry into force of the imposed restrictions to individual motion inside the country during the period between March and April 2020, we report also the positive side effects which are reflected on the resulting acoustic environment.

Among the 24 sites, three of them have been taken as an example to highlight the differences between the "normal" reference period (from 23rd March 2019 to 3rd May 2019) and the extraordinary period linked to Covid-19 lockdown (from 23rd March 2020 to 3rd May 2020).

These three sites belong to two different clusters, with a low (x = 1.13; cluster 2), intermediate (x = 3.94, value very close to the separation threshold between the two clusters; cluster 2) and high (x = 4.85; cluster 1) non-acoustic parameter, according to the classification of a "normal" period. The first is characterized by the presence of an urban local road (Via Leonardo Bruni), surrounded by a school and residential buildings (Figure 1).

The second site is characterized by the presence of an urban local road (Via Crespi), surrounded by a school, residential buildings, a chemical industry and a park (Figure 2).

The third is a representative site near an arterial thoroughfare characterized by high capacity traffic flows (Viale Enrico Fermi) in the proximity of Niguarda hospital (on the right side of Figure 3).

Figure 1: Google Earth's view illustrating the position of hb139 sensor (Group (a))

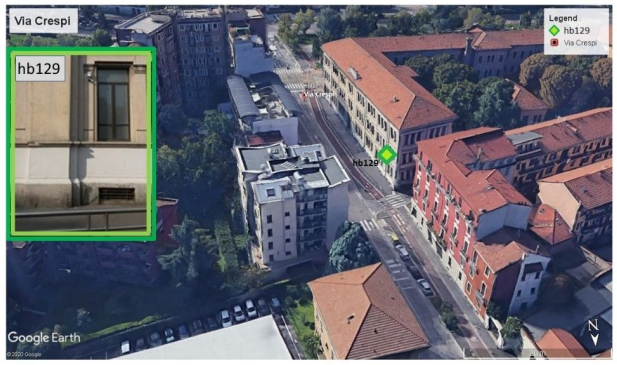

Figure 2: Google Earth's view illustrating the position of hb129 sensor (Group (a))

Figure 3: Google Earth's view illustrating the position of hb117 sensor (Group (b))

Figures 4-6 (Left panel) display the hourly median daily profile calculated during lockdown and the same period in 2019 for the monitoring sensors hb139, hb129 and hb117, respectively. For all monitoring sites, the correction due to façade reflections reported in ISO 1996-2 standard has not been applied. This means that, as most of the mi-

crophones are installed flush with the wall, a –6 dBA correction needs to be applied to Figures 4-6.

For the monitoring sensor hb139, the mean noise reduction is by about 5.4 dB with a minimum of 2 dB at 5:00 (IQR of about 8 dB; high variability due to local fluctuations) and a maximum of 9.6 dB at 23:00. For the monitoring sensor hb129, the mean noise reduction is by about 6.1 dB with a minimum of 3.6 dB at 4:00 and a maximum of 10.4 dB at 23:00, and for hb117, the mean noise reduction is by about 6.1 dB with a minimum of 2.8 dB at 4:00 and a maximum of 9.8 dB at 23:00. This result underlines a reduced traffic flow during the whole day (presence of just essential services and activities) and a complete absence of nightlife. To be noted, the high inter-quartile range (IQR) recorded for hb139 sensor: a mean value of 3.5 dB for 2020 against 2.3 dB for 2019. This high variability is typical of local roads where very few vehicles passing by may impact significantly. Conversely, hb129 and hb117's IQR is far more stable for the two years with a mean value of approximately (1.2-2.0) dB. Table 3 reports the mean, minimum and maximum noise reduction and the corresponding time of the day between reference and lockdown periods for each monitoring station. These results show that the mean noise reduction ranges between 3.4 and 8.5 dB with minima concentrated between the night and early morning (4:00-7:00) and maxima in the late evening.

Figures 4-6 (Right panel) show the timeline of the equivalent noise level calculated over the daytime, $LAeq_{06-22}$, for the reference period and lockdown for the three considered monitoring stations. The timeline is quite irregular with a mean reduction over the entire considered period of 5.3, 5.0 and 5.8 dB for sensor hb139, hb129 and hb117, respectively. Irregularities are more likely due to local daily fluctuations. Also for this case, a –6 dB correction needs to be applied.

3.1 Noise pattern stability across the monitoring network

One of the main results of DYNAMAP project is the strict link between traffic noise patterns and traffic volumes [22]. This consideration prompted us to analyse the radical changes triggered by the restriction imposed to mobility in the country which has been heavily impacted by the pandemic of Covid-19.

As already mentioned in the Introduction, the European project DYNAMAP [20] has been developed to implement a dynamical acoustic map in two pilot areas: a large portion of the urban area of the city of Milan (Area 9) [18] and the motorway surrounding Rome [16]. In particular, in the urban area of Milan a statistical survey and a specific algorithm have been implemented in order to predict the traffic noise in an extended area using a limited number of monitoring sensors and the knowledge of a so called non-acoustic parameter based on vehicular rate. In particular, the statistical analysis revealed that roads can be grouped into two clusters, each one reflecting different traffic noise patterns [22].

In order to decide whether the conditions of applicability of DYNAMAP's updating algorithm were still valid, we compared the noise trends recorded by all the monitoring stations during lockdown (23rd March- 3rd May 2020) and the reference period (23rd March- 3rd May 2019). From this dataset, we removed all anomalous noise event not due to traffic noise sources [24, 25] and we excluded all festivities, weekends, rainy and windy days as described in Sect. 2.

The outcome of the "clValid" R-package performed on the available median profiles (21 for 2019 and 22 for 2020), yielded the following ranking (Table 3):

- 2019 median profiles:
    1) Hierarchical with Ward algorithm with two clusters,
    2) DIANA with two clusters,
    3) AGNES with two clusters.
- 2020 median profiles:
    1) Hierarchical with Ward algorithm with two clusters,
    2) AGNES with two clusters,
    3) k-means with five clusters.

Table 4 reports the clustering membership obtained by applying the Hierarchical clustering with Ward algorithm with two clusters to both the 2019 and 2020 dataset. The table also reports the information regarding the monitoring sensors, the corresponding non-acoustic parameter x, together with cluster memberships in the reference period of "normal" activity and during lockdown. The results show that in the latter case the 22 monitoring sensors do not follow the distribution into the two clusters obtained for the reference period. They also show that for the 2019 dataset the sensors are quite well distributed in the two clusters with 11 sensors belonging to cluster 1 and 10 sensors to cluster 2. This result underlines the robustness of the clustering method and the stability of the traffic noise profiles as already found in the original sampling measurements taken over the entire city and in a previous work devoted to the analysis of the accuracy of DYNAMAP predictions [23].

The results obtained for the lockdown dataset show that the two clusters are less balanced (8 sensors belong to cluster 1 and 14 to cluster 2). Moreover, calculating the

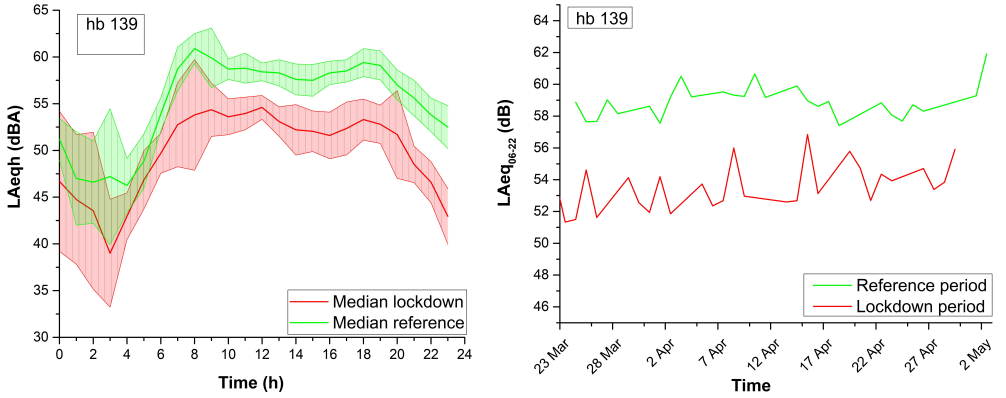

Figure 4: (Left panel) Hourly 24h median LAeqh profile calculated during lockdown and the same period of 2019 for the monitoring sensor hb139. Hb139 belongs to cluster 2 (Group (a)) with x=1.13 (see Table 4). The coloured bands represent the inter-quartile range. (Right panel) Timeline of the equivalent noise level calculated over the daytime, $LAeq_{06-22}$, for the reference period and lockdown. The correction due to façade reflections reported in ISO 1996-2 standard has not been applied. This means that a −6 dBA correction needs to be applied

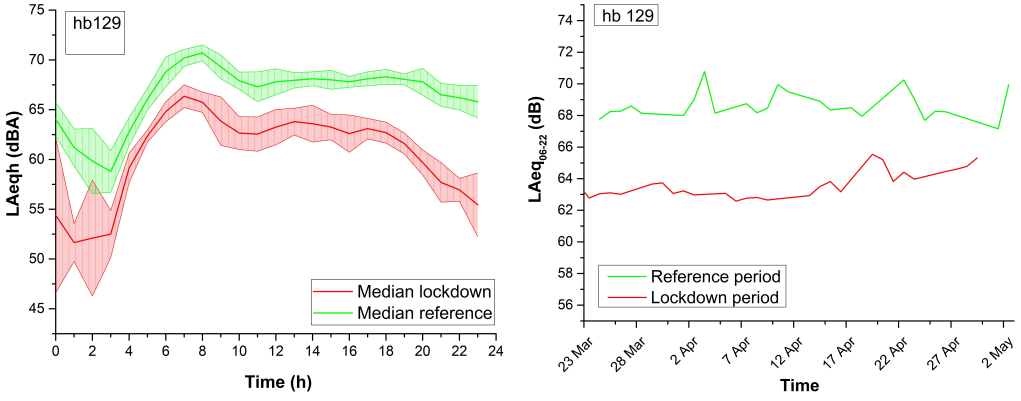

Figure 5: (Left panel) Hourly 24h median LAeqh profile calculated during lockdown and the same period of 2019 for the monitoring sensor hb129. Hb129 belongs to cluster 2 (Group (a)) with $x = 3.94$ (see Table 4). The coloured bands represent the inter-quartile range. (Right panel) Timeline of the equivalent noise level calculated over the daytime, $LAeq_{06-22}$, for the reference period and lockdown. The correction due to façade reflections reported in ISO 1996-2 standard has not been applied. This means that a −6 dBA correction needs to be applied

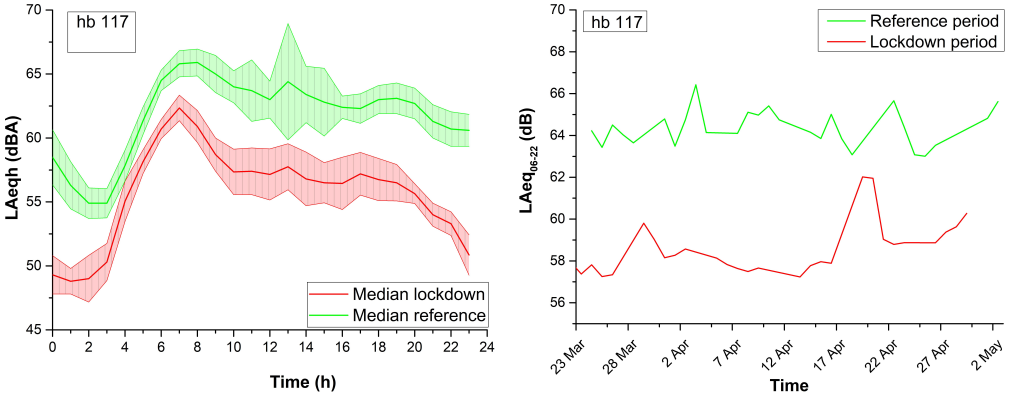

Figure 6: (Left panel) Hourly 24h median LAeqh profile calculated during lockdown and the same period of 2019 for the monitoring sensor hb117. Hb117 belongs to cluster 1 (Group (b)) with $x = 4.85$ (see Table 4). The coloured bands represent the inter-quartile range. (Right panel) Timeline of the equivalent noise level calculated over the daytime, $LAeq_{06-22}$, for the reference period and lockdown. The correction due to façade reflections reported in ISO 1996-2 standard has not been applied. This means that a −6 dBA correction needs to be applied

Table 3: Mean, minimum and maximum noise reduction and the corresponding time of the day between reference and lockdown periods for each monitoring station

Site	Sensor code	Mean noise reduction [dB]	Minimum noise reduction [dB] Hour	Maximum noise reduction [dB] Hour
Via Litta Modignani	hb106	3.4	1.8 07:00	6.1 00:00
Via Piero e Alberto Pirelli (U4)	hb108	7.1	4.3 06:00	12.1 23:00
Viale Stelvio	hb109	4.8	3.1 06:00	7.1 23:00
Via Melchiorre Gioia	hb114	6.9	3.6 05:00	10.2 23:00
Via Fara	hb115	6.7	4.3 06:00	9.3 23:00
Via Moncalieri	hb116	5.3	1.5 05:00	10.1 00:00
Viale Fermi	hb117	6.1	2.8 04:00	9.8 23:00
Via Baldinucci	hb120	4.9	2.6 12:00	8.7 01:00
Via Piero e Alberto Pirelli (U6)	hb121	5.3	2.7 01:00	6.8 03:00
Via Abba	hb125	7.1	4.6 04:00	11.5 23:00
Via Quadrio	hb127	8.5	3.7 05:00	12.2 23:00
Via Crespi	hb129	6.1	3.6 04:00	10.4 23:00
Via Maffucci	hb133	5.7	3.3 05:00	10.3 23:00
Via Lambruschini	hb135	5.9	−0.1 04:00	11.3 18:00
Via Comasina	hb136	3.5	2.0 03:00	7.0 23:00
Via Maestri del lavoro	hb137	3.2	1.3 01:00	5.5 19:00
Via Novaro	hb138	4.9	2.6 04:00	9.0 23:00
Via Bruni	hb139	5.4	2.0 05:00	9.6 23:00
Viale Jenner	hb140	4.5	2.3 07:00/08:00/13:00	9.7 00:00
Via D'Intignano	hb144	6.8	0.9 05:00	13.4 13:00
Via Fratelli Grimm	hb145	6.1	3.2 05:00	9.4 23:00
Via Veglia	hb151		N.A.	

Table 4: Monitoring sensor information: code, non-acoustic parameter, $x = \log T_t$, mean total number of vehicles in a day, T_t, cluster membership for the reference year (2019) and during lockdown. N.A. non-available

Sensor Code	$x=\log T_t$	T_t (vehicles/day)	Cluster membership 2019	Cluster membership 2020
hb139	1.13	13	2	2
hb137	1.9	79	2	2
hb125	2.69	490	2	2
hb135	2.89	776	2	1
hb144	2.94	871	2	2
hb108	3.06	1148	1	2
hb145	3.42	2630	2	2
hb115	3.58	3802	2	2
hb116	3.6	3981	2	1
hb120	3.74	5495	1	2
hb133	3.75	5623	2	2
hb106	3.9	7943	1	1
hb127	3.9	7943	1	2
hb129	3.94	8710	1	1
hb121	4.06	11482	1	2
hb138	4.19	15488	2	1
hb136	4.21	16218	1	1
hb151	4.4	25119	N.A.	1
hb114	4.58	38019	1	2
hb140	4.7	50119	1	2
hb109	4.75	56234	1	2
hb117	4.85	70795	1	1

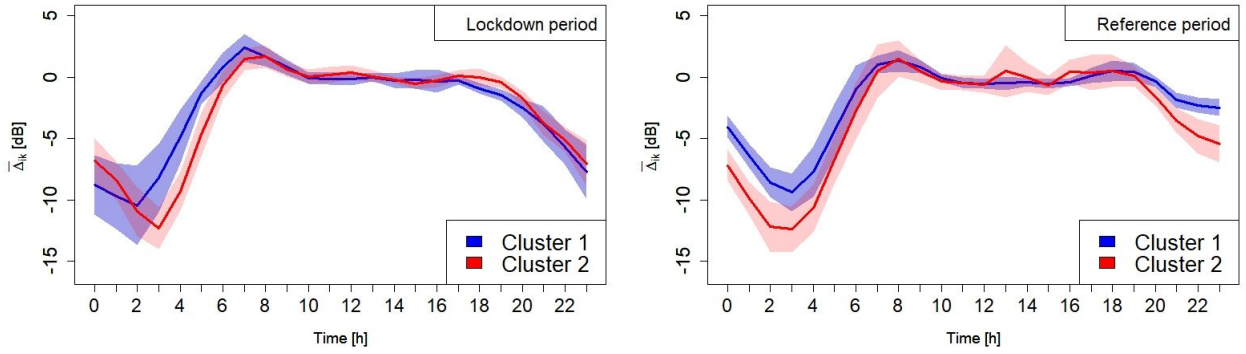

Figure 7: Mean normalized cluster profiles, $\overline{\Delta_k}$, and the corresponding error band for lockdown (left panel) and for the reference period (right panel); k indicates the cluster index ($k = 1, 2$). Time resolution $\tau = 1$ hour. The coloured band represents the spread of the sample distribution around the mean value (sample standard deviation s). In these calculations, the normalized noise level is obtained following the procedure described in Sect. 2

Spearman's correlation coefficient between the two ranked variables, it yields a value of 0.067 showing the complete absence of correlation between the two clustering results referring to 2019 and 2020 dataset.

In Figure 7 we report the mean hourly normalized cluster profiles, $\overline{\Delta_k}$, and the corresponding error band for lockdown (left panel) and for the reference period (right panel); k indicates the cluster index ($k = 1, 2$). The coloured band represents the spread of the sample distribution (sample standard deviation s). In this case, the main difference is found in the evening and night periods where the effect of lockdown, prohibiting hangouts, produced a complete reshaping of the noise patterns.

Regarding the statistical independence between the two cluster samples, a nonparametric Mann-Whitney-Wilcoxon's (MWW) test has been applied to the two distri-

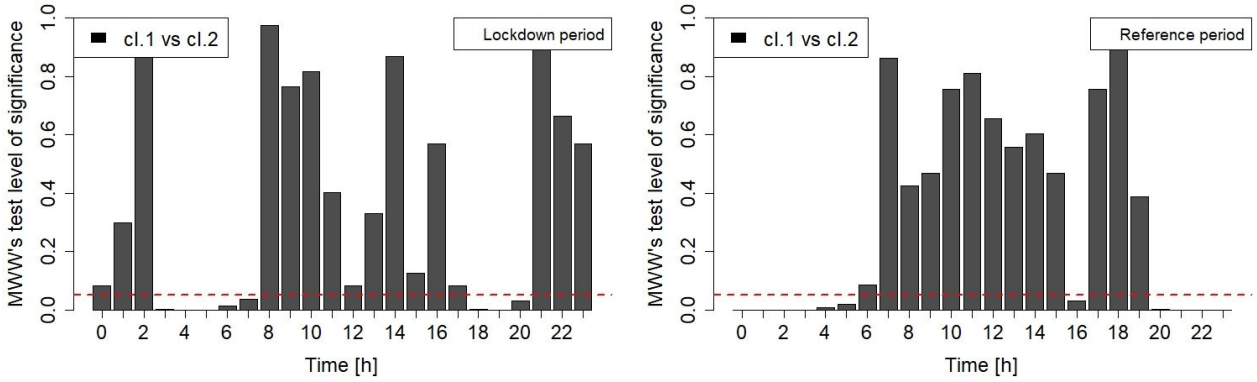

Figure 8: Two-tailed p-values results from Wilkoxon-Man-Whitney (MMW) test for the two clusters obtained for: (Left panel) Lockdown; (Right panel) Reference period

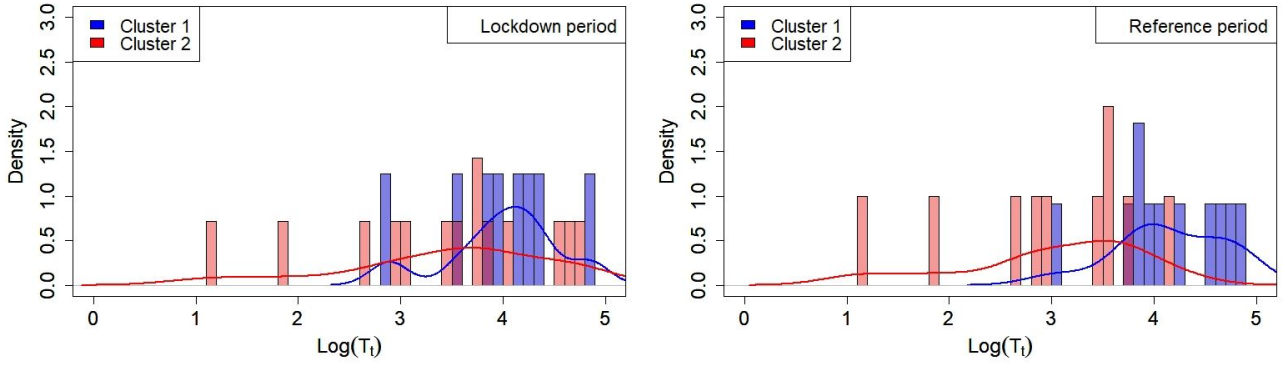

Figure 9: Histograms and density distributions as a function of the non-acoustic parameter, x, for Cluster 1 and 2 obtained from the 22 monitoring stations for lockdown period (left panel) and the 21 monitoring stations for the reference period (right panel). Bin size is 0.1

butions in Figure 5 (left and right panels, separately). The two-tailed p-values for both tests are illustrated in Figure 6. The reference value set at $\alpha = 0.05$ significance level, corresponding to 95% confidence level, has been drawn to help interpret the results. Figure 8 (left panel) shows that the two mean profiles result statistically distinct for eight hours along the day (hours: from 3:00 to 7:00 and from 18:00 to 20:00), whereas for the right panel, they result statistically distinct for eleven hours along the day (hours: from 20:00 to 5:00 and at 16:00).

These results seem to confirm that the effect of lockdown is to smooth the differences in terms of noise profiles among the monitoring sites. Such differences were mainly concentrated during the night period for the reference period, whereas during lockdown they get further reduced. Figure 9 illustrates the histograms and density distributions as a function of the non-acoustic parameter, x, for Cluster 1 and 2, obtained from the 22 monitoring stations during lockdown (left panel) and the 21 monitoring stations for the reference period (right panel). Also in this case, we can appreciate the spreading of the monitoring stations belonging to the two clusters over the non-acoustic range underlying the changes of noise patterns. To be noted that the non-acoustic parameter used for this analysis is related to the model calculations of the traffic flow on the whole road network of Milan. Such calculations refer to a "normal" activity period. They have been also applied to lockdown period just for a comparison but cannot be used to identify a threshold value of x to discriminate between the two clusters.

Therefore, these results suggest that the algorithm developed to calculate and update the dynamic noise map (DYNAMAP), following the procedure described in the Introduction, *i.e.* the predictive capability of DYNAMAP based on the stationarity of the traffic noise profiles, is no longer applicable during lockdown because of the change of the traffic noise dynamic characteristics over the entire road network.

4 Conclusions

In Italy, lockdown started on 23rd March, 2020 and extended until 3rd May, 2020. The extraordinary restrictive regulation brought to a prohibition of all non-essential commercial activities, businesses and industries. Consequently, the acoustic environment in all cities changed dramatically. The presence of a permanent noise-monitoring network in the urban area of Milan, developed in the framework of DYNAMAP project, allowed capturing this acoustic variation by comparing the sound levels recorded during lockdown and a reference period (23rd March – 3rd May 2019). The noise recorded at three sites (in correspondence of the noise monitoring station hb139, hb129 and hb117) shows a mean reduction of about 6 dB.

Most important is the change in the dynamic behaviour of the traffic noise. This arose in the different clustering results obtained on the median normalized hourly levels, recorded by the monitoring stations in the two periods of study. The obtained clusters differ both by composition and pattern. The Spearman's correlation coefficient between the two ranked variables, yields a value of 0.067 showing the complete absence of correlation between the two clustering results. Therefore, these results suggest that the algorithm developed to predict the noise levels over an extended area must be reconsidered and adapted to the new traffic noise pattern configuration to be applicable during an extraordinary situation, such as that of lockdown. The accuracy of DYNAMAP prediction during lockdown could not be quantified due to the restrictions in individual mobility, preventing us from performing test measurements of traffic noise. As going back to a pre-lockdown situation seems to take a long time, the time evolution of the noise profiles will need to be continuously monitored in order to attribute to DYNAMAP the pre-lockdown accuracy.

Conflict of Interests: The authors declare no conflict of interest regarding the publication of this paper.

References

[1] EU Directive (2002), Directive 2002 /49/EC of the European parliament and the Council of 25 June 2002 relating to the assessment and management of environmental noise, Official Journal of the European Communities, L189/12, July 2002.

[2] World Health Organization (WHO) Environmental noise guidelines, 2018. Website: https://www.euro.who.int/en/health-topics/environment-and-health/noise/publications/2018/environmental-noise-guidelines-for-the-european-region-executive-summary-2018. (accessed on 30 September 2020)

[3] Arana M., Martin R.S., Nagore I., Perez D., Main results of strategic noise maps and action plans in Navarre (Spain). Environ. Monit. Assess., 2013, 185(6), 4951-4957.

[4] Paschalidou A.K., Kassomenos P., Chonianaki F., 3-year noise monitoring and strategic noise mapping in an extended motorway, Sci. Total Environ., 2019, 654, 144-153.

[5] Klaeboe R., Engelien E., Steinnes M., Context sensitive noise impact mapping, Appl. Acoust., 2006, 67 620-642.

[6] COM/2017/0151 final. European Commission 2017. Report From The Commission To The European Parliament And The Council On the Implementation of the Environmental Noise Directive in accordance with Article 11 of Directive 2002/49/EC.

[7] Licitra G., Noise mapping in the EU, CRC Press, 2012.

[8] Kang J., Aletta F., Gjestland T.T., Brown L.A., Botteldooren D., Schulte-Fortkamp B., Lercher P., van Kamp I., Genuit K., Fiebig A., Bento Coelho J.L., Maffei L., Lavia L., Ten questions on the soundscapes of the built environment, Build. and Environ., 2016, 108, 284-294.

[9] Aumond P., Jacquesson L., Can A., Probabilistic modeling framework for multisource sound mapping, Appl. Acoust., 2018,139, 34-43.

[10] Guarnaccia C., Quartieri J., Analysis of road traffic noise propagation, Int. J. Math. Models Meth. Appl. Sci., 2012, 6, 926-933.

[11] Zambon G., Roman H.E., Benocci R., Vehicle speed recognition from noise spectral patterns, Int. J. Environ. Res., 2017, 11(4), 449-459.

[12] Zambon G., Roman H.E., Benocci R., Scaling model for a speed-dependent vehicle noise spectrum, Journal of Traffic and Transportation Engineering (English Edition), 2017, 4(3), 230-239.

[13] Brambilla G., Confalonieri C., Benocci R., Application of the intermittency ratio metric for the classification of urban sites based on road traffic noise events, Sensors, 2019, 19, 23.

[14] Brambilla G., Benocci R., Confalonieri C., Roman H.E., Zambon G., Classification of Urban Road Traffic Noise based on Sound Energy and Eventfulness Indicators, Appl. Sci., 2020,10, 2451.

[15] Manvell D., Ballarin Marcos L., Stapelfeldt H., Sanz R., SADMAM-Combining Measurements and Calculations to Map Noise in Madrid. In Proceedings of the Inter-Noise 2004, Prague, Czech Republic, 22-25 August 2004.

[16] Benocci R., Bellucci P., Peruzzi L., Bisceglie A., Angelini F., Confalonieri C., Zambon G., Dynamic Noise Mapping in the Suburban Area of Rome (Italy), Environments, 2019, 6(7), 79.

[17] de Coensel B., Sun K., Wei W., van Renterghem T., Sineau M., Ribeiro C., Can A., Aumond P., Lavandier C., Botteldooren D., Dynamic noise mapping based on fixed and mobile sound measurements, EURONOISE 2015, Maastricht, Pays-Bas, 2015-06-01, 6.

[18] Benocci R., Molteni A., Cambiaghi M., Angelini F., Roman H.E., Zambon G. Reliability of DYNAMAP traffic noise prediction, Appl. Acoust., 2019, 156, 142-150.

[19] Wei W., Van Renterghem T., De Coensel B., Botteldooren D., Dynamic noise mapping: A map-based interpolation between noise measurements with high temporal resolution, Appl. Acoust., 2016, 101, 127-140.

[20] DYNAMAP. 2014. Available online: http://www.life-dynamap.eu/it (accessed on 30 September 2020).

[21] Barrigón Morillas J.M., Gómez Escobar V., Méndez Sierra J.A., Vílchez-Gómez R., Vaquero J.M., Trujillo Carmona J., A categorization method applied to the study of urban road traffic noise, J.

Acoust. Soc. Am., 2005, 117, 2844-2852.
[22] Gozalo G.R., Barrigón Morillas J.M., Escobar V.G., Analyzing nocturnal noise stratification, Science of the Total Environ., 2014, 479, 39-47.
[23] Gozalo G.R., Barrigón Morillas J.M, Prieto Gajardo C., Urban noise functional stratification for estimating average annual sound level, J. Acoust. Soc. Am., 2015, 137(6), 3198-3208.
[24] Zambon G., Benocci R., Bisceglie A., Roman H.E., Milan dynamic noise mapping from few monitoring stations: Statistical analysis on road network, Proceedings of the INTER-NOISE 2016 - 45th International Congress and Exposition on Noise Control Engineering: Towards a Quieter Future, 6350-6361.
[25] Zambon G., Benocci R., Bisceglie A., Roman H.E., Bellucci P., The LIFE DYNAMAP project: Towards a procedure for dynamic noise mapping in urban areas, Appl. Acoust., 2017, 124, 52-60.
[26] Benocci R., Confalonieri C., Roman H. E., Angelini F., Zambon G., Accuracy of the dynamic acoustic map in a large city generated by fixed monitoring units, Sensors, 2020, 20, 412.
[27] R.M. Alsina-Pagès, F Alías, J.C. Socoró, F. Orga, R. Benocci, G. Zambon, Anomalous events removal for automated traffic noise maps generation, Appl. Acoust., 2019, 151, 183-192.
[28] Orga F., Socoró J.C., Alías F., Alsina-Pagès R.M., Zambon G., Benocci R., Bisceglie A., Anomalous noise events considerations for the computation of road traffic noise levels: The DYNAMAP's Milan case study, 24th International Congress on Sound and Vibration, ICSV 2017.
[29] ISO 1996-2: 2017. Description, measurement and assessment of environmental noise. Part 2: determination of sound pressure levels. Switzerland: International Organization for Standardization; 2017.
[30] Montes González D. Barrigón Morillas J.M. Rey Gozalo G. Atanasio Moraga P. Microphone position and noise exposure assessment of building façades, Appl. Acoust., 2020, 160, 107157.
[31] Ward J.H., Hierarchical Grouping to Optimize an Objective Function, J. Amer. Statist. Assoc., 1963, 58, 236-244.
[32] Hartigan J.A., Wong M.A., A K-means clustering algorithm, Appl. Statist., 1979, 28, 100-108.
[33] Kaufman L., Rousseeuw P., Finding Groups in Data, Wiley Series in Probability and Mathematical Statistics, 1990.
[34] Herrero J., Valencia A., Dopazo J., A hierarchical unsupervised growing neural network for clustering gene expression patterns, Bioinformat., 2005, 17, 126-136.
[35] R Core Team , R: A language and environment for statistical computing, R Foundation for Statistical Computing, 2015, Vienna, Austria. Available at: https://www.r-project.org/ (accessed on 30 September 2020).
[36] Brock G., Pihur V., Datta S., Datta S., clValid: An R Package for Cluster Validation, J. Statist. Software, 2008, 25, 1-22.
[37] Package "clValid" version 0.6-4, 2013; Available at: https://cloud.r-project.org/web/packages/clValid/clValid.pdf. (accessed on 30 September 2020)
[38] Pihur V., Datta S., Datta S., Weighted rank aggregation of cluster validation measures: a Monte Carlo cross-entropy approach, Bioinformat., 2007, 23, 1607-1615.
[39] Rousseeuw P.J., Silhouettes: A Graphical Aid to the Interpretation and Validation of Cluster Analysis, J. Comput. Appl. Math., 1987, 20, 53-65.
[40] Datta S., Datta S., Comparisons and Validation of Statistical Clustering Techniques for Microarray Gene Expression Data, Bioinformat., 2003, 19, 459-466.
[41] Dunn J.C. Well Separated Clusters and Fuzzy Partitions, J. Cybernet., 1974, 4, 95-104.
[42] Handl J., Knowles J., Kell D.B., Computational Cluster Validation in Post-Genomic Data Analysis, Bioinformat., 2005, 21, 3201-3212.
[43] Yeung K.Y., Haynor D.R., Ruzzo W.L., Validating Clustering for Gene Expression Data, Bioinformat., 2001, 17, 309-318.